

## PERFORMANCE ANALYSIS OF P&O AND PSO MPPT ALGORITHMS FOR PV SYSTEMS UNDER PARTIAL SHADING

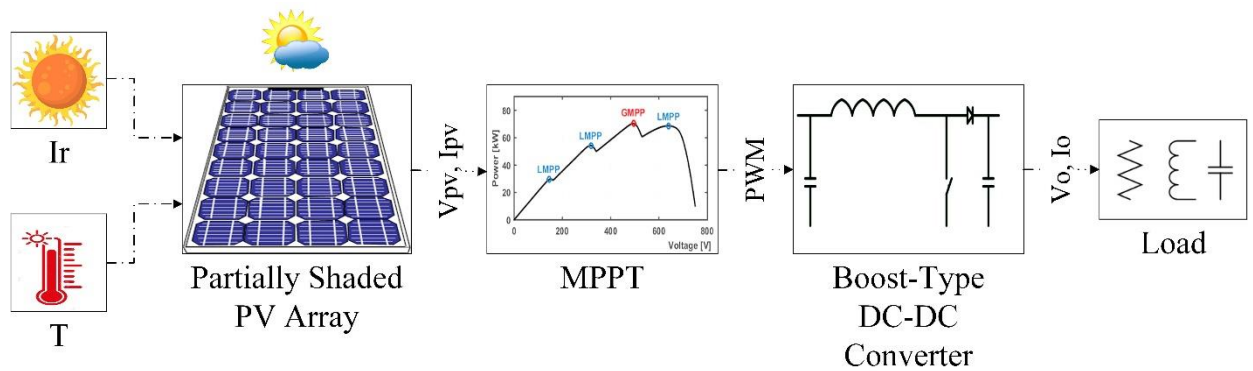
\*Mustafa Sacid ENDİZ 

*Necmettin Erbakan University, Engineering Faculty, Electrical-Electronics Department, Konya, TÜRKİYE*  
[mSENDIZ@ERBAKAN.EDU.TR](mailto:mSENDIZ@ERBAKAN.EDU.TR)

### Highlights

- Modeling and simulation of the designed PV system applying P&O and PSO MPPT strategies.
- Performance analysis under uniform and two different partial shading configurations.
- Discussing the results based on tracking efficiency and convergence speed of the MPPT system.

### Graphical Abstract



Graphical abstract of the proposed system.



## PERFORMANCE ANALYSIS OF P&O AND PSO MPPT ALGORITHMS FOR PV SYSTEMS UNDER PARTIAL SHADING

\*Mustafa Sacid ENDİZ 

*Necmettin Erbakan University, Engineering Faculty, Electrical and Electronics Department, Konya, TÜRKİYE*  
[msendiz@erbakan.edu.tr](mailto:mSENDIZ@ERBAKAN.EDU.TR)

(Received: 12.09.2023; Accepted in Revised Form: 22.12.2023)

**ABSTRACT:** Photovoltaic (PV) modules are devices that transform photon energy into electrical energy. The output power of the PV modules is influenced by the intensity of solar radiation and the ambient temperature. Non-uniform shading can cause variations in the extent of sunlight absorbed by PV modules, resulting in a decrease in power output. Maximum power point tracking (MPPT) techniques are employed to optimize the power output of PV modules by operating them at their maximum power point (MPP). The main objective of the study is to investigate the performance analysis of Perturb and Observe (P&O) and Particle Swarm Optimization (PSO) MPPT strategies in uniform and partially shaded conditions with equally and unequally different irradiance differences. Simulation studies were conducted on the PV circuit model using Matlab/Simulink, and the results were evaluated. MPPT algorithms are compared based on their tracking efficiency and convergence speed when solar radiation conditions vary. The findings of the simulation indicate that the P&O is unable to determine global MPP and gets trapped in one of the local MPPs. However, the PSO is very effective in tracking MPP under different partial shading patterns with more than 96% tracking efficiency. In the first partial shading configuration where the sunlight intensity of the PV modules is uniformly distributed, the PSO technique has reduced steady-state oscillations around the MPP. However, the P&O technique demonstrates superior response time and convergence speed in comparison to the PSO technique.

**Keywords:** MPPT, P&O, Partial shading, Photovoltaic, PSO

### 1. INTRODUCTION

The global demand for energy generation is experiencing a significant increase due to population and economic growth, with fossil fuels emerging as the dominating source. The environmental impact of greenhouse gas emissions from burning fossil fuels and the fact that these fuels will be depleted in the near future due to the limited reserves increase the need for clean and infinite energy sources [1]. Countries are turning to the use of renewable energy resources that produce very low or near zero greenhouse gas emissions to respond to increasing energy demands and prevent global warming. Therefore, the significance of environmentally friendly and cost-effective renewable energy sources is growing rapidly [2-4].

Due to its low cost, ease of use, and ecologically beneficial characteristics, the use of solar power in electricity production has grown rapidly in recent years. Solar energy can be directly transformed into direct current (DC) electricity using photovoltaic (PV) technology [5]. PV modules are composed of PV cells that are interconnected in series and parallel, and a PV array consists of PV modules. PV cells are the smallest part of a solar power system and are made up of semiconductor material. In a PV cell, sunlight is converted into electrical energy by absorbing the energy in the photon particles, which is commonly referred to as the photovoltaic effect. When a PV cell is subjected to solar radiation, it causes electron movement, resulting in the generation of a voltage potential across the front and back surfaces of the cell. Thus, a solar cell can produce an electric current [6, 7].

The solar radiation value reaching the Earth's atmosphere is accepted as approximately 1000W/m<sup>2</sup> due to the losses and reflections of the photon particles. PV modules used today provide energy conversion

\*Corresponding Author: Mustafa Sacid ENDİZ, [msendiz@erbakan.edu.tr](mailto:mSENDIZ@ERBAKAN.EDU.TR)

with an efficiency between 15% and 20% depending on the cell structure despite all current technological developments. Therefore, it is significant to use PV modules with the highest possible efficiency. PV module output power varies depending on the solar radiation intensity and ambient temperature during the day [8]. The current of a PV module exhibits a proportionate change in response to an increase in solar radiation intensity. Consequently, the module's output power experiences a rise. As the ambient temperature rises, there is a corresponding increase in the current value of the PV module, while the voltage value decreases. Since the change in PV voltage value is greater than the current change, the overall power output of the PV module decreases. The technique known as maximum power point tracking (MPPT) refers to the process of maintaining the output power of a PV module at its highest achievable level [9]. The achievement of the highest power output in PV systems occurs at a specific operating point referred to as the Maximum Power Point (MPP). Independent of environmental conditions, with MPPT techniques the PV module is continuously operated at the maximum available power point. The position of this point varies continually in response to changes in environmental conditions.

### 1.1. Literature Review

Several MPPT methods are discussed in literature studies, however, they all have their drawbacks when it comes to PV applications in terms of efficiency, cost, and usability [10, 11]. MPPT techniques use two different methods, direct and indirect search, to obtain the MPP. The direct methods depend on variations in current and voltage values, while the indirect methods search the MPP with solar radiation, temperature, and certain mathematical expressions. In the last few years, metaheuristic optimization MPPT algorithms have been proposed which can dynamically track the real MPP [12]. Due to the bypass diodes, in addition to the global MPP, the power-voltage curve of a PV module exhibits many local MPPs as a result of the non-uniform shading effect. In the presence of a non-uniform shading effect, in addition to a global MPP, there are multiple local MPPs in the power-voltage curve of the PV module due to the bypass diodes. The commonly used MPPT techniques are not sufficient to track the MPP in normal conditions as well as in conditions of partial shading. However, metaheuristic optimization algorithms can effectively track the MPP in both cases, so that they can avoid getting trapped in local MPPs [13]. The PV array must always operate at the global MPP to maximize energy generation. A study presents a hybrid MPPT technique using Particle Swarm Optimization (PSO) and Perturb and Observe (P&O) methods for PV systems. Simulations show the proposed technique can track global MPP under uniform and partial shading conditions, with a 50% shorter tracking time and 0.3% more electricity extraction [14]. Another study introduces a logarithmic PSO method for MPPT, reducing power oscillations and accelerating convergence without search space reduction. In the steady-state process, the swarm is reduced to a single particle, which slightly changes to detect local variations [15]. A study compares P&O and PSO algorithms for MPPT in PV power systems. The results show that P&O is faster but generates significant energy losses due to constant oscillations. PSO is slower but less energy-intensive, and only PSO ensures convergence to the MPP under partial shading conditions [16]. Three MPPT algorithms, P&O, Incremental Conductance (INC), and PSO are compared to show the effectiveness in PV systems. While the P&O and INC are simple to implement, the PSO is more effective in optimizing the output power [17]. This study investigates the performance analysis of P&O and PSO MPPT techniques in uniform and partially shaded conditions with equally and unequally different irradiance differences based on the tracking efficiency and convergence speed on the designed PV circuit model developed in Matlab/Simulink. The rest of the paper is structured as follows: Section 2 explains a single-diode PV cell model with mathematical expressions, the details of the P&O and PSO algorithms, and the boost-type DC-DC converter respectively. Section 3 describes the parameters of the developed PV system and discusses the simulation results. Section 4 outlines conclusions and suggestions for further study.

## 2. MATERIAL AND METHODS

### 2.1. A Single-diode PV Cell Model

The solar cell, consisting of P-type and N-type semiconductor materials, is the smallest unit in PV systems that directly transforms the absorbed solar radiation into electricity. Photons of varying energy levels make up solar radiation, and part of these photons are absorbed in the p-n junction. Solar energy is transformed into DC electricity by combining photons with energies higher than the band gap of semiconductor material to the electrons in the atoms. PV modules are formed at the desired power values by combining solar cells appropriately. The PV cell's single-diode model, which is used more frequently than the two-diode model because of its ease of usage and reasonable accuracy, is shown in Figure-1. On the equivalent circuit model of the PV cell,  $I_{ph}$  is the current generated by the PV cell,  $I_d$  is the diode current,  $I_p$  is the current of the parallel resistance,  $I_{pv}$  is the output current of the PV cell,  $D$  is the diode,  $R_p$  is the resistance parallel to the current source,  $R_s$  is the series connected resistance, and  $R_L$  is the output load resistance [18].

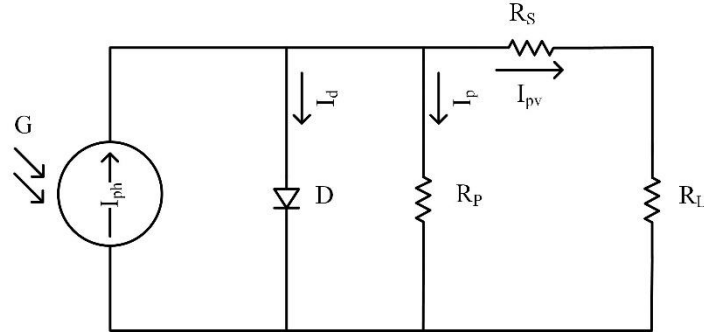


Figure 1. The single-diode model of the PV cell

Solar radiation ( $G$ ) and cell temperature ( $T$ ) are directly related to the production of electricity from sunlight. Equation 1 and Equation 2 indicate the generated current  $I_{ph}$  and the output current  $I_{pv}$  respectively. In the below equations;  $I_{sc}$  is the short circuit current at 25 °C and 1000W/m<sup>2</sup>,  $K_i$  is the temperature coefficient of the short circuit current, and  $\Delta T$  is the difference between reference temperature and PV cell temperature.

$$I_{ph} = [I_{sc} + K_i * \Delta T] \frac{G}{G_r} \quad (1)$$

$$I_{pv} = I_{ph} - I_d - I_p \quad (2)$$

### 2.2. Perturb and Observe (P&O) MPPT Technique

MPPT algorithms are employed to regulate the operating point of the PV array at its MPP. The complexity, tracking speed, accuracy, oscillations, and hardware implementation of these techniques differ among themselves. Many different algorithms have been proposed in recent years as potential approaches to MPP tracking. One of the most frequently employed MPPT strategies among the traditional MPPT techniques is the P&O technique. The fundamental concept underlying this methodology is to track the changes in module output power. The operating point is determined by checking the module's power-voltage curve and slope ( $dP/dV$ ) variation as shown in Figure-2. A positive derivative of power to voltage indicates that the operating point is to the left of the MPP. Conversely, a negative slope shows that the operating point is to the right of the power-voltage curve. By adjusting the duty ratio, the P&O continually changes the voltage level of the PV array to approach the MPP [19].

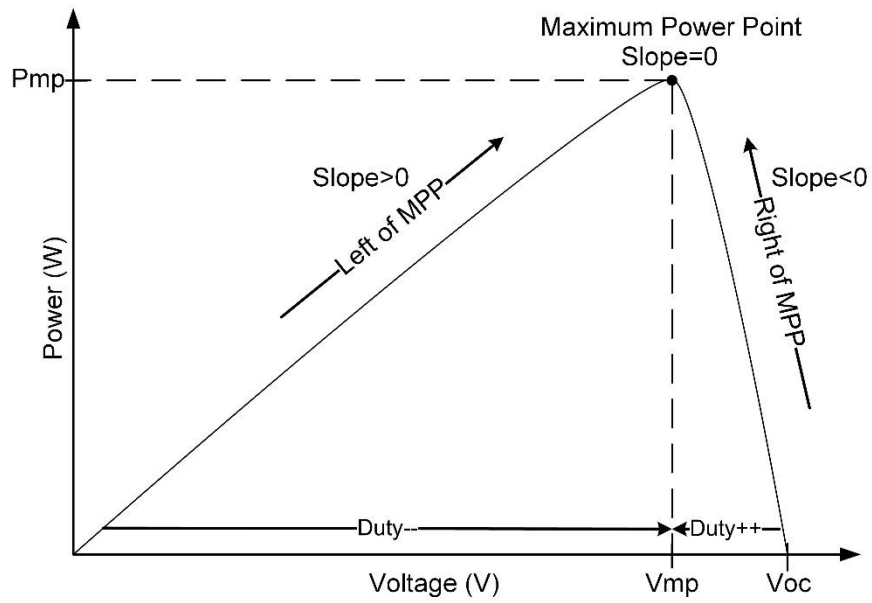


Figure 2. Behavior of the P&O MPPT with P-V curve

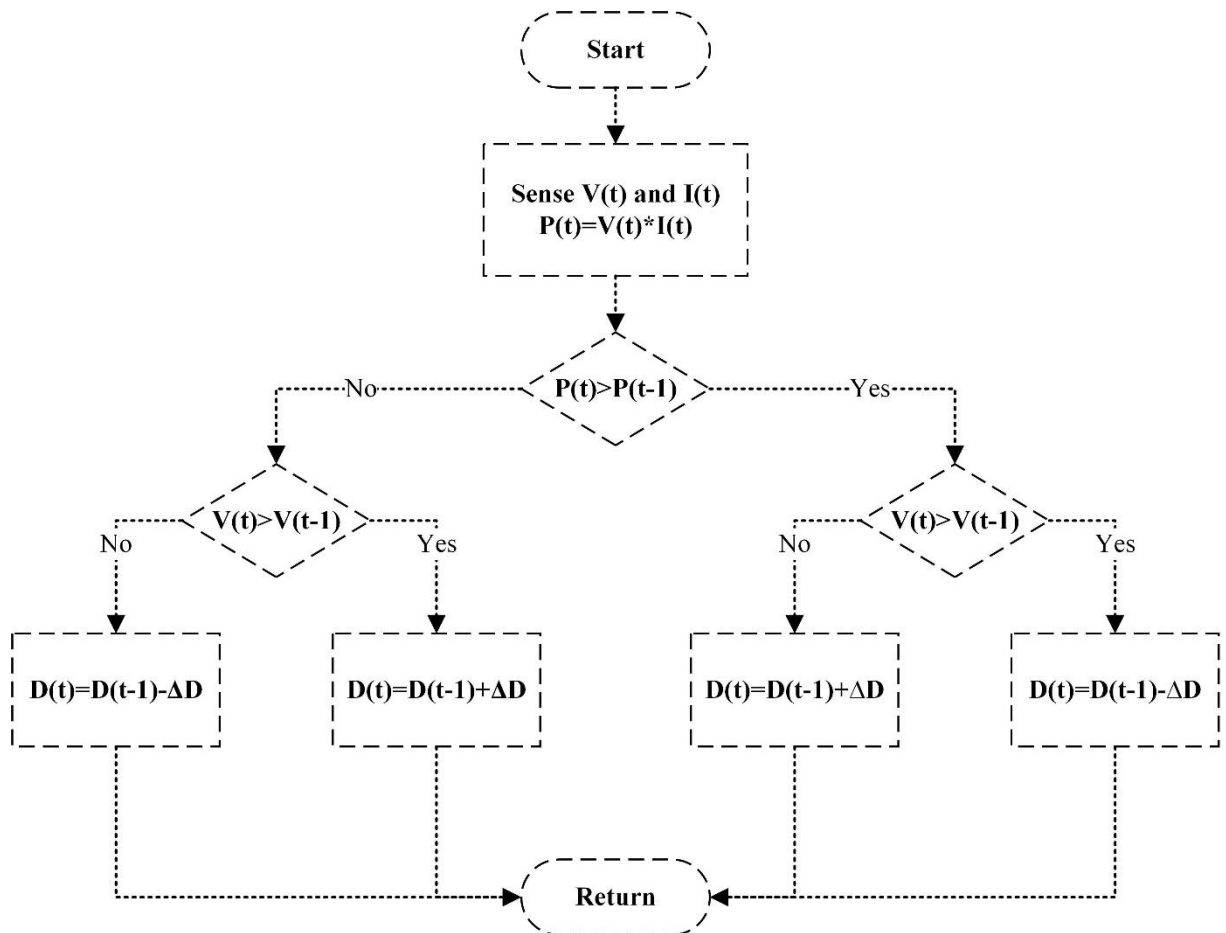


Figure 3. Flowchart of the P&O MPPT algorithm

In Figure-3, the flowchart of the P&O MPPT is demonstrated. The P&O technique's primary limitations are its inefficiency in quickly changing air conditions and its significant steady-state oscillations around the MPP due to the continual repetition of the perturbation process in both directions. For PV module operation, the P&O typically uses a constant step size interval. However, using a constant

step size speeds up tracking but causes high steady-state oscillations at the MPP. This can be solved by damping the oscillations, which slows tracking. Variable step sizes can be used in the algorithm to improve tracking performance and reduce high steady-state oscillations. The P&O based on the variable step-size algorithm can improve the tracking performance. Because of its simple structure and potential for improvement, P&O MPPT is widely used [19].

### 2.3. Particle Swarm Optimization (PSO) MPPT Technique

In recent years, metaheuristic optimization algorithm based MPPT approaches have become increasingly popular due to their many advantages over conventional MPPT algorithms. Especially, under partial shade conditions, the MPP is not tracked by conventional approaches due to the existence of several power peaks in the P-V characteristics curve. The PSO algorithm was introduced by Eberhart and Kennedy in 1995 as a population-based metaheuristic intelligent optimization approach which is characterized by its simplicity and effectiveness [20]. The basic idea of the algorithm was based on how groups of birds move together to solve problems in the search process and optimization. The flowchart of the PSO MPPT is depicted in Figure-4.

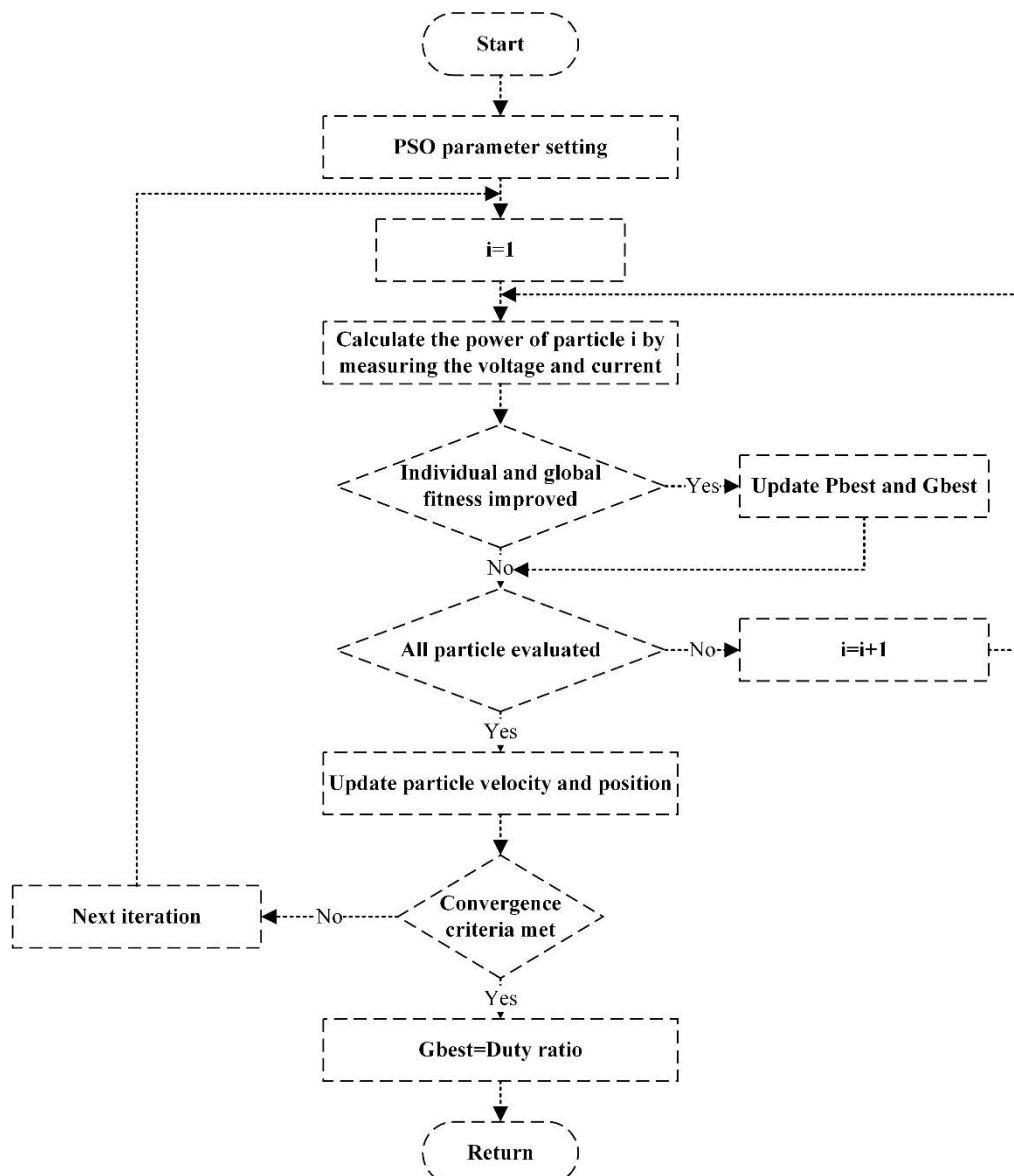


Figure 4. Flowchart of the PSO MPPT algorithm

Each particle in the PSO algorithm's population represents a distinct approach to the optimization issue. During the search process of the algorithm, the particles in the swarm continuously update their velocity and position to iteratively determine the optimal solution. Each particle communicates with its neighbors, evaluates points in a D-dimensional search space, and moves according to its best individual position ( $P_{best}$ ) and the global best position ( $G_{best}$ ). Thus,  $P_{best}$  and  $G_{best}$  have a role in determining where each particle is located. This leads to the swarm converging rapidly on the best possible solution. The position and velocity for each article are updated using the following equations:

$$x_i^{k+1} = x_i^k + \Phi_i^{k+1} \quad (3)$$

$$\Phi_i^{k+1} = w\Phi_i^k + c_1r_1\{P_{best} - x_i^k\} - c_2r_2\{G_{best} - x_i^k\} \quad (4)$$

Where  $x_i$  and  $\Phi_i$  are the position and velocity of each particle (i) respectively,  $k$  is the iteration counter,  $w$  is the inertia weight,  $c_1$  and  $c_2$  are acceleration factors,  $r_1$  and  $r_2$  are random values that are evenly spread between 0 and 1. The fitness value of each particle is determined using the output voltage and output current of the PV array, which is denoted as the power of the PV array. The highest produced power is considered the best in the population. The PSO search process terminates after the maximum number of iterations has been achieved. In particular, when facing non-uniform solar irradiation, the use of the PSO MPPT improves the performance of the PV array and offers the greatest available amounts of power [21].

### 2.3. Boost-type DC-DC Converter

To maximize the output power of the PV module in a wide range of conditions, MPPT algorithms regulate the duty ratio of the PWM signal that is sent to the switch of the power conversion stage. As a high-frequency power conversion circuit between the PV array and the load, a boost-type converter is employed to increase the input voltage to higher values [22, 23].

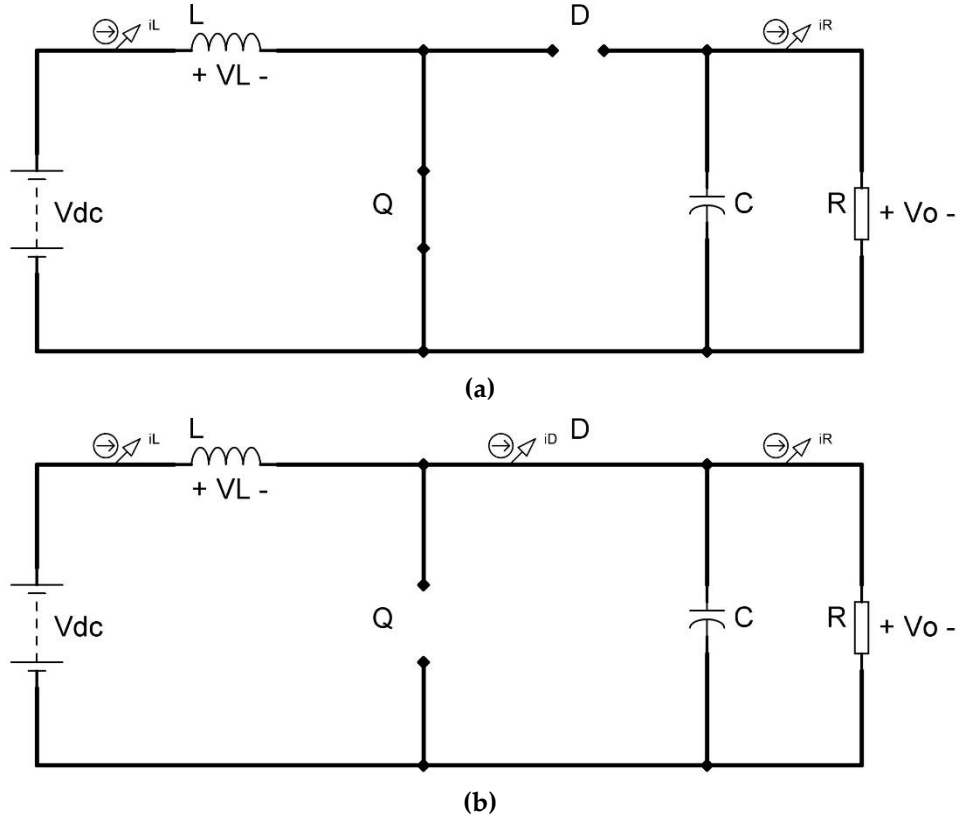


**Figure 5.** A boost-type DC-DC converter a) On state b) Off state

As illustrated in Figure-5, a boost-type converter consists of circuit components including a diode, an inductor, a capacitor, and a semiconductor switch. To step up DC voltage from its input, a boost-type converter has the capability of being operational in either a continuous or discontinuous conduction mode during the switching process. Because of the switching device's lower peak current and conduction losses, continuous conduction mode operation is more widely used. This can be achieved by selecting the appropriate inductor and capacitor values. During switching states, the output load receives a higher voltage because of the energy stored in the inductor's magnetic field. By adjusting the duty ratio of the PWM signal, the output voltage of the boost-type converter can be determined [22]. As given in Equation (5), the output voltage of the boost converter is proportional to its duty ratio. Equation (6) and Equation (7) are used to determine minimum inductor ( $L_{min}$ ) and capacitor ( $C_{min}$ ) values for the desired ripple current and output voltage ripple [24, 25]. In the below equations,  $V_{dc}$  is input voltage,  $V_o$  is output voltage,  $\Delta D$  is duty ratio,  $\Delta V_o$  is output voltage ripple,  $i_o$  is output current,  $\Delta i_L$  is inductor ripple current, and  $f$  is the switching frequency.

$$\frac{V_o}{V_{dc}} = \frac{1}{1-\Delta D} \quad (5)$$

$$L_{min} = \frac{V_{dc}(V_o - V_{dc})}{\Delta i_L f V_o} \quad (6)$$

$$C_{min} = \frac{i_o \Delta D}{f \Delta V_o} \quad (7)$$

### 3. RESULTS AND DISCUSSION

PSO and P&O MPPT techniques are compared based on tracking efficiency and convergence speed. Simulations are conducted on the developed Matlab/Simulink model, which is shown in Figure-6. The PV circuit model consists of a partially shaded PV array comprised of four series-connected PV modules of

250 W, a boost-type DC-DC converter with MPPT controller, and a DC load. Figure-7 depicts the PV array current-voltage curve for different solar radiations. Table 1 and Table 2 list the irradiance-temperature data, and the parameters of the selected PV module respectively. In Table 3, the specifications of the designed boost-type converter are listed for the required inductor ripple current and output voltage ripple at the switching frequency of 5 kHz.

At standard test conditions (1000 W/m<sup>2</sup> of sunlight; 25 °C cell temperature), for the boost-type converter the input voltage is 122.8 V, the output voltage is 225 V, the input current is 8.75 A, the output current is 4.25 A, and the output power is 955 W. The initial duty ratio of the boost-type converter for P&O and PSO MPPT is set to 0.1 and 0.5 respectively. Using Equation (5), Equation (6), and Equation (7), the maximum available duty ratio is 0.45, and minimum inductor ( $L_{min}$ ) and capacitor ( $C_{min}$ ) values are 1 mH and 470 uF respectively. The effectiveness of the PSO algorithm is dependent on the settings of its various parameters. In the swarm, the number of particles is 4, the number of iterations  $k=300$ , the inertia weight  $w=0.4$ , the acceleration factors  $c1=1.2$ , and  $c2=2$ .

In terms of performance analysis, P&O and PSO MPPT approaches are compared with uniform and two different partial shading configurations. In Figure-8, the PV array configurations under partial shading are depicted. Figure-9 shows the P-V curve under uniform and partial shading conditions. Both MPPT techniques are tested first at standard test conditions and then at two different partial shading conditions. While the solar radiation levels of the first pattern are 400 W/m<sup>2</sup>, 600 W/m<sup>2</sup>, 800 W/m<sup>2</sup>, and 1000 W/m<sup>2</sup>, the second pattern consists of 1000 W/m<sup>2</sup>, 900 W/m<sup>2</sup>, 700 W/m<sup>2</sup>, and 400 W/m<sup>2</sup> at constant temperature (25 °C). When comparing the two different patterns for the partial shading conditions, it can be noticed that the irradiance difference of the PV modules in the first pattern is equally different from each other (200 W/m<sup>2</sup>) while it is variable in the second pattern.

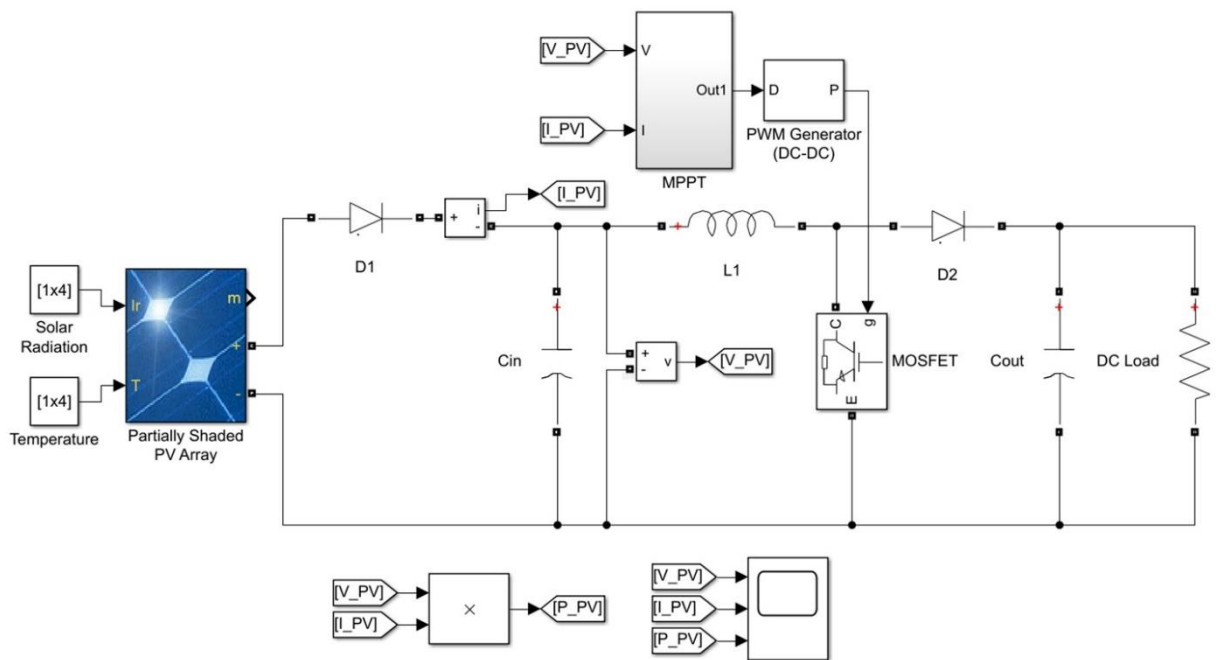
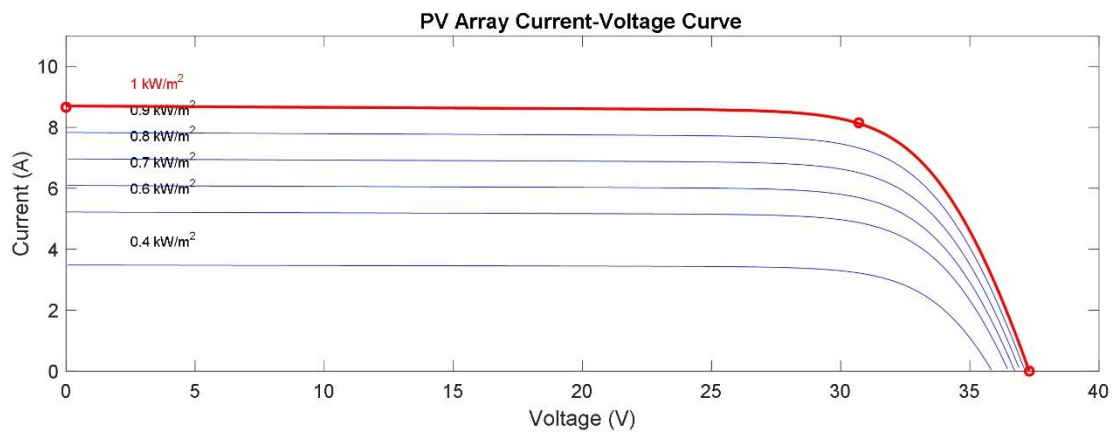


Figure 6. Matlab/Simulink model of the presented system

**Table 1.** The irradiance-temperature data

Irradiance (W/m <sup>2</sup> )	Temperature (°C)
<b>First pattern</b>	
400 W/m <sup>2</sup>	25 °C
600 W/m <sup>2</sup>	25 °C
800 W/m <sup>2</sup>	25 °C
1000 W/m <sup>2</sup>	25 °C
<b>Second pattern</b>	
1000 W/m <sup>2</sup>	25 °C
900 W/m <sup>2</sup>	25 °C
700 W/m <sup>2</sup>	25 °C
400 W/m <sup>2</sup>	25 °C

**Figure 7.** PV array current-voltage curve for different solar radiations

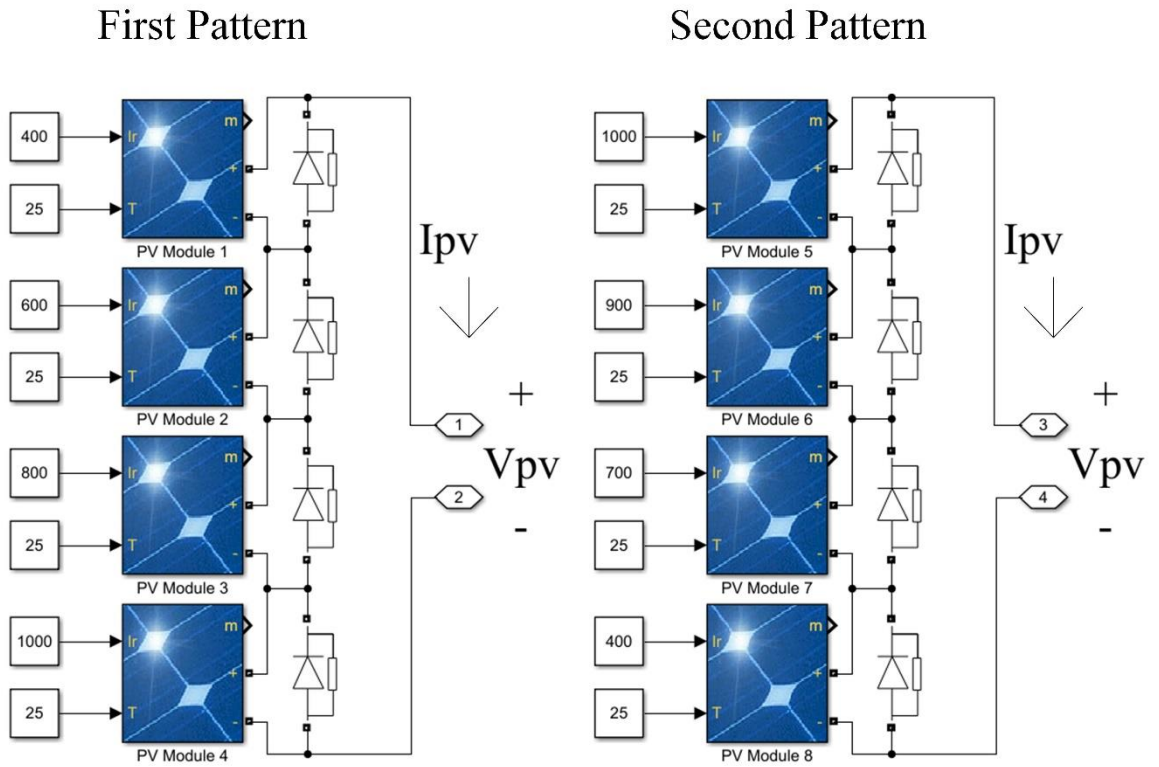


Figure 8. Patterns for partial shading conditions

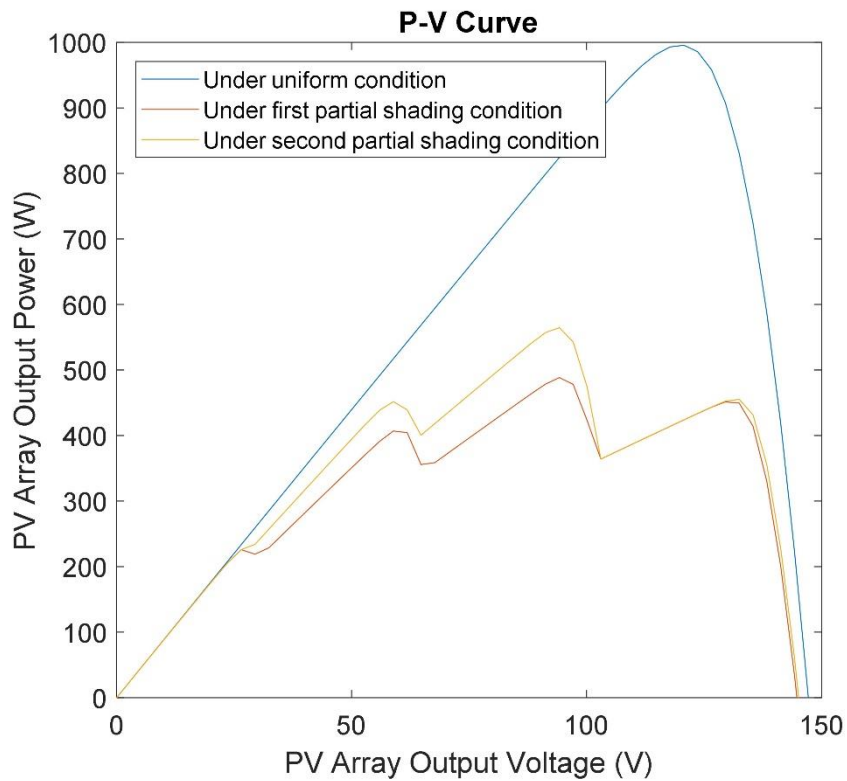


Figure 9. P-V Curve under uniform and partial shading conditions

**Table 2.** PV module parameters

Parameters	Values
Series-connected modules per string	4
Parallel strings	1
Cells per module (Ncell)	60
Maximum power (W)	250
Voltage at maximum power point $V_{mp}$ (V)	30.7
Current at maximum power point $I_{mp}$ (A)	8.15
Open circuit voltage $V_{oc}$ (V)	37.3
Short-circuit current $I_{sc}$ (A)	8.66
Temperature coefficient of $V_{oc}$ (%/deg.C)	-0.36901
Temperature coefficient of $I_{sc}$ (%/deg.C)	0.086998

**Table 3.** Boost-type converter specifications

Parameters	Values
Load resistance ( $\Omega$ )	50
Inductance (mH)	1
Capacitance ( $\mu$ F)	470
Switching frequency (kHz)	5
Inductor current ripple $\Delta i_L$	%10
Capacitor voltage ripple $\Delta V_o$	%2

**Figure 10.** Duty cycle change for the P&O and PSO

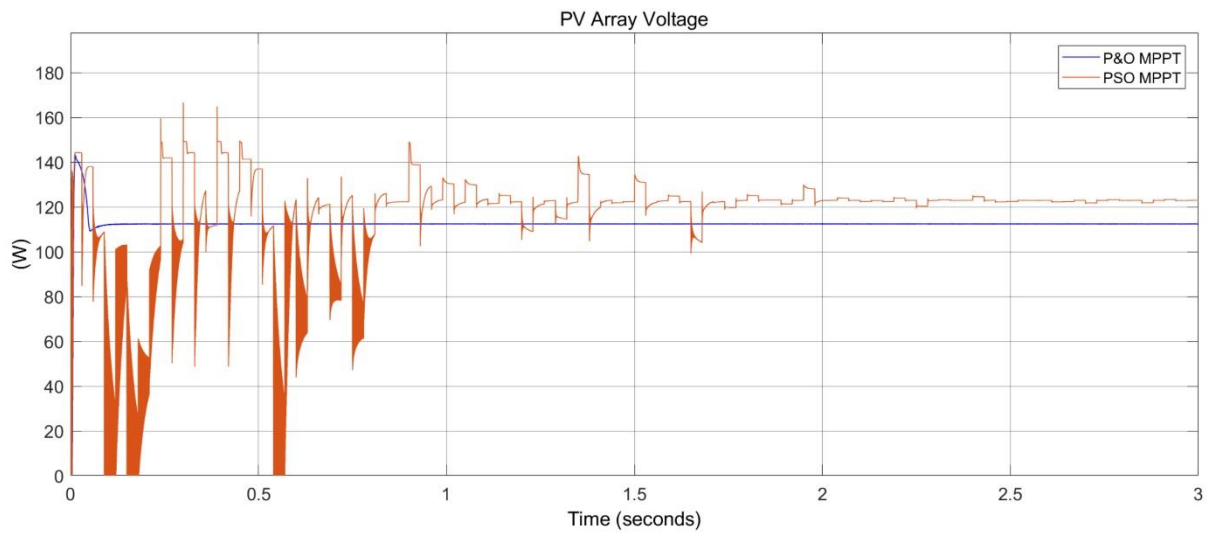


**Figure 11.** PV array voltage for the P&O and PSO

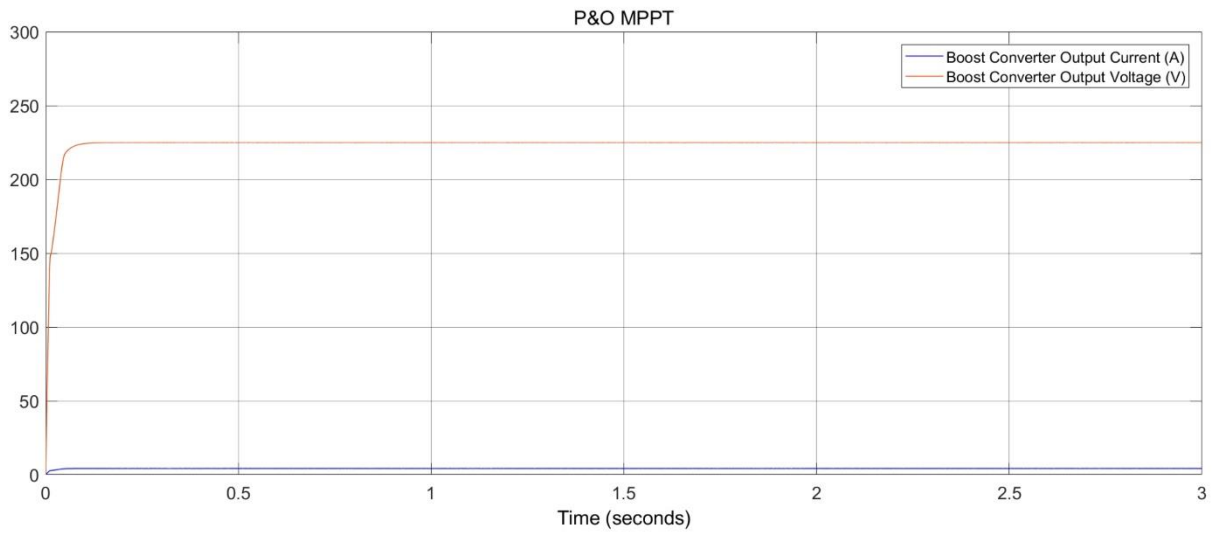


**Figure 12.** Boost-type DC-DC converter output current and voltage for the P&O

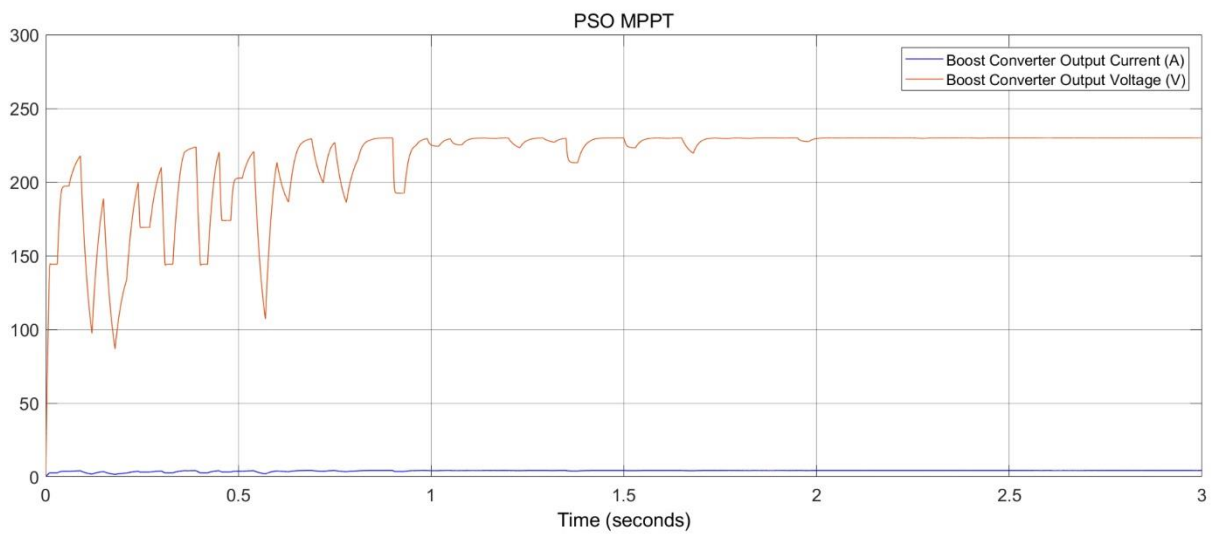


**Figure 13.** Boost-type DC-DC converter output current and voltage for the PSO

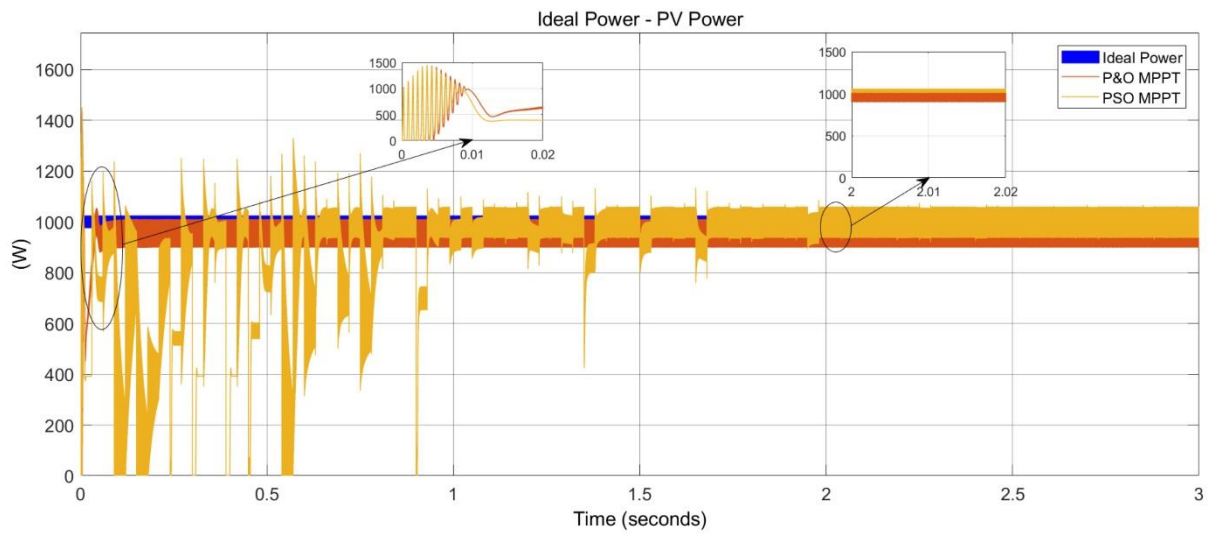


Figure 14. PV array power for the P&O and PSO at standard test conditions

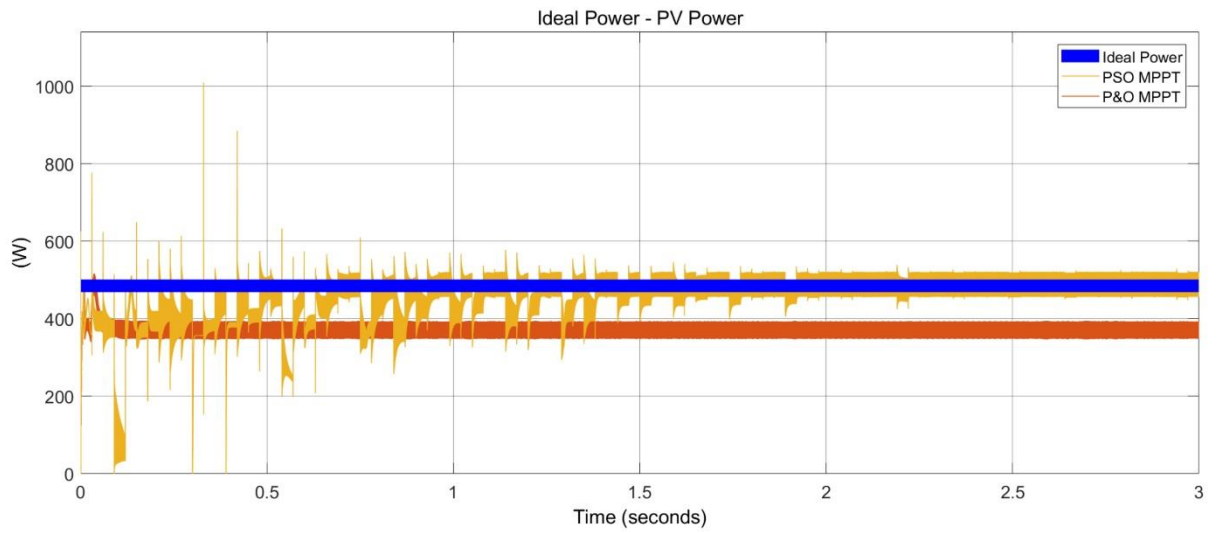


Figure 15. PV array power for the P&O and PSO at the first partial shading condition

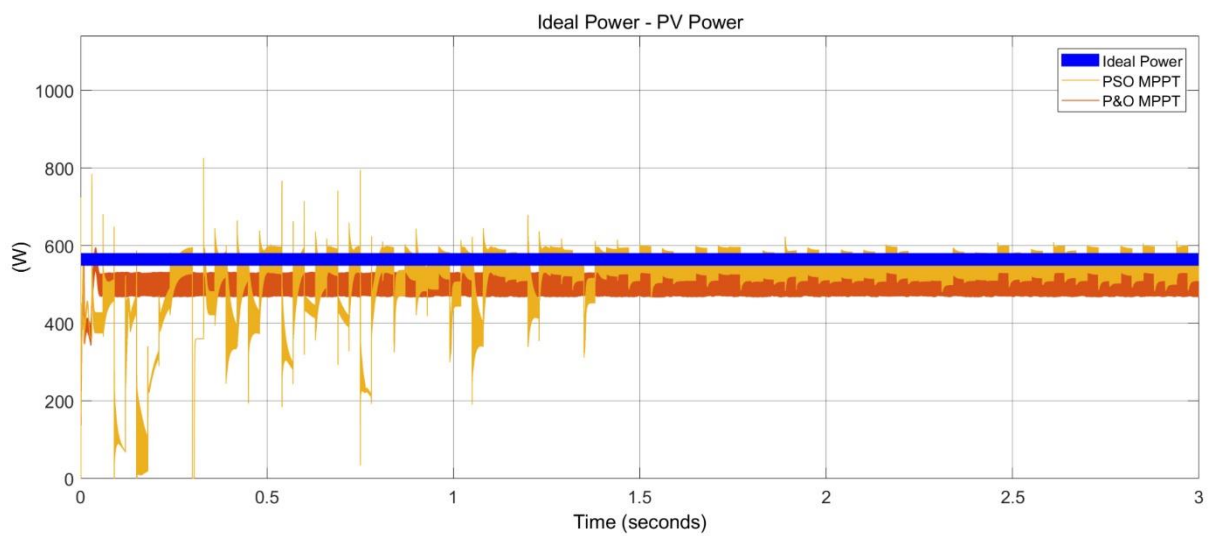


Figure 16. PV array power for the P&O and PSO at the second partial shading condition

PSO and P&O MPPT techniques are tested for 3 seconds on the Matlab/Simulink-based PV circuit model. Duty cycle change, PV array voltage, boost-type DC-DC converter output current and voltage, and PV array power for the P&O and PSO in uniform and partially shaded conditions with equally and unequally different irradiance differences are given in between Figures-10-16 respectively. As shown in Figure-14, both MPPT techniques are capable of tracking MPP under standard test conditions. However, while the PO technique stays at 980 W, the PSO technique reaches a power of 986 W during the search process. On the other hand, PSO is relatively slow in reaching the MPP compared to the P&O. The PSO algorithm caught the MPP in 1.65 seconds, while the P&O algorithm reached this in 0.2 seconds. Although the PSO is a widely used optimization algorithm for tracking the global MPP, it has power ripple and slow convergence speed due to its unique characteristics such as large search space and huge computing efforts during the search process.

Partial shading conditions cause non-uniform shading and different irradiance levels in PV arrays. The decrease in solar radiation on the surface of the PV module leads to a corresponding reduction in the total power output of the PV array. When the simulation results of the first partial shading configuration are examined as shown in Figure-15, P&O is trapped in one of the local MPPs but PSO has demonstrated considerable performance in finding the global MPP. The P&O algorithm stays at 380 W, while the PSO algorithm has a power output of 478 W.

In the second partial shading configuration as shown in Figure-16, P&O again failed to track global MPP and gets trapped in one of the local MPPs. PSO, on the other hand, is quite successful in finding the global MPP. Both MPPT techniques reach 485 W and 545 W MPP values respectively. Similar to the results of the standard test condition, P&O reveals a superior response time with 0.2 seconds and fast convergence in the presence of partial shading too. The PSO technique reaches the global MPP in 1.8 seconds and 1.5 seconds for two different partial shading conditions respectively. Compared to the previous studies, the main difference of this study is that, it observes partially shaded conditions with equal and unequal irradiance differences. When comparing the two different patterns for the partial shading conditions, it can be seen that the PSO technique has lower steady-state oscillations at the MPP in the first configuration where the sunlight intensity of the PV modules is equally different from each other. Based on the simulation results, the mean values of PV array power, tracking efficiency, and convergence speed for P&O and PSO are listed in Table 4.

**Table 4.** PV array power, tracking efficiency, convergence speed, and response time for P&O and PSO

Condition	MPPT	PV Array Power (W)	Tracking Efficiency (%)	Convergence Speed	Response Time (s)
Standard Test Condition	P&O	980	98	Fast	0.2
	PSO	986	98.6	Moderate	1.65
First Partial Shading Condition	P&O	380	76.5	Fast	0.2
	PSO	478	96.5	Moderate	1.8
Second Partial Shading Condition	P&O	485	85.8	Fast	0.2
	PSO	545	96.4	Moderate	1.5

#### 4. CONCLUSIONS

The tracking efficiency and convergence speed of the P&O and PSO MPPT algorithms are compared on the designed PV circuit model built in Matlab/Simulink. Under uniform and two different partial shading configurations, the simulations are conducted. P&O and PSO techniques are successful in finding the MPP under uniform solar radiation. Under partial shading configurations, however, P&O gets trapped in the local MPP, where PSO has approached the global MPP. Regarding convergence speed, the P&O

technique is quite fast in uniform and partially shading conditions while the PSO technique takes more time to converge to global MPP. Furthermore, it can be seen that the PSO technique has reduced steady-state oscillations around the MPP in the first partial shading configuration where the irradiance difference of the PV modules is uniformly distributed. Future studies can be conducted to overcome the main limitations of the PSO technique such as longer response time to reach the maximum power and higher transient and steady-state oscillations around the MPP.

### Declaration of Ethical Standards

The author declares to comply with all ethical guidelines, including authorship, citation, data reporting, and original research publication.

### Declaration of Competing Interest

The author declares that he has no known competing financial interests or personal relationships that could have appeared to influence the work reported in this paper.

### Funding / Acknowledgements

The author declares that he has not received any funding or research grants during the review, research, or assembly of the article.

### Data Availability

Data will be made available on request.

### REFERENCES

- [1] X. Zheng, D. Streimikiene, T. Balezentis, A. Mardani, F. Cavallaro, and H. Liao, "A review of greenhouse gas emission profiles, dynamics, and climate change mitigation efforts across the key climate change players," *Journal of Cleaner Production*, vol. 234, pp. 1113-1133, 2019.
- [2] A. Qazi *et al.*, "Towards sustainable energy: a systematic review of renewable energy sources, technologies, and public opinions," *IEEE access*, vol. 7, pp. 63837-63851, 2019.
- [3] S. R. Sinsel, R. L. Riemke, and V. H. Hoffmann, "Challenges and solution technologies for the integration of variable renewable energy sources—a review," *renewable energy*, vol. 145, pp. 2271-2285, 2020.
- [4] C. Gao and H. Chen, "Electricity from renewable energy resources: Sustainable energy transition and emissions for developed economies," *Utilities Policy*, vol. 82, p. 101543, 2023.
- [5] E. Kabir, P. Kumar, S. Kumar, A. A. Adelodun, and K.-H. Kim, "Solar energy: Potential and future prospects," *Renewable and Sustainable Energy Reviews*, vol. 82, pp. 894-900, 2018.
- [6] B. Parida, S. Iniyar, and R. Goic, "A review of solar photovoltaic technologies," *Renewable and sustainable energy reviews*, vol. 15, no. 3, pp. 1625-1636, 2011.
- [7] N. Sharma and V. Puri, "Solar energy fundamental methodologies and its economics: A review," *IETE Journal of Research*, vol. 69, no. 1, pp. 378-403, 2023.
- [8] A. Karafil, H. Ozbay, and M. Kesler, "Temperature and solar radiation effects on photovoltaic panel power," *Journal of New Results in Science*, vol. 5, pp. 48-58, 2016.
- [9] S. Motahhir, A. El Hammoumi, and A. El Ghzizal, "The most used MPPT algorithms: Review and the suitable low-cost embedded board for each algorithm," *Journal of cleaner production*, vol. 246, p. 118983, 2020.
- [10] N. Karami, N. Moubayed, and R. Outbib, "General review and classification of different MPPT Techniques," *Renewable and Sustainable Energy Reviews*, vol. 68, pp. 1-18, 2017.

- [11] F. A. Omar, G. Gökkuş, and A. A. KULAKSIZ, "ŞEBEKEDEN BAĞIMSIZ FV SİSTEMDE MAKSİMUM GÜÇ NOKTASI TAKİP ALGORİTMALARININ DEĞİŞKEN HAVA ŞARTLARI ALTINDA KARŞILAŞTIRMALI ANALİZİ," *Konya Journal of Engineering Sciences*, vol. 7, no. 3, pp. 585-594, 2019.
- [12] Z. Salam, J. Ahmed, and B. S. Merugu, "The application of soft computing methods for MPPT of PV system: A technological and status review," *Applied energy*, vol. 107, pp. 135-148, 2013.
- [13] H. Rezk, A. Fathy, and A. Y. Abdelaziz, "A comparison of different global MPPT techniques based on meta-heuristic algorithms for photovoltaic system subjected to partial shading conditions," *Renewable and Sustainable Energy Reviews*, vol. 74, pp. 377-386, 2017.
- [14] S. Figueiredo and R. N. A. L. e Silva, "Hybrid mppt technique pso-p&o applied to photovoltaic systems under uniform and partial shading conditions," *IEEE Latin America Transactions*, vol. 19, no. 10, pp. 1610-1617, 2021.
- [15] S. Makhloufi and S. Mekhilef, "Logarithmic PSO-based global/local maximum power point tracker for partially shaded photovoltaic systems," *IEEE Journal of Emerging and Selected Topics in Power Electronics*, vol. 10, no. 1, pp. 375-386, 2021.
- [16] O. M. Elbadri, K. M. Mohammed, and Z. I. Saad, "Comparison of P&O and PSO Algorithms using Matlab/Simulink," in *The 7th International Conference on Engineering & MIS 2021*, 2021, pp. 1-7.
- [17] H. El Hammedi, J. Chroua, H. Khaterchi, and A. Zaafouri, "Comparative study of MPPT algorithms: P&O, INC, and PSO for PV system optimization," in *2023 9th International Conference on Control, Decision and Information Technologies (CoDIT)*, 2023: IEEE, pp. 2683-2688.
- [18] A. M. Humada, M. Hojabri, S. Mekhilef, and H. M. Hamada, "Solar cell parameters extraction based on single and double-diode models: A review," *Renewable and Sustainable Energy Reviews*, vol. 56, pp. 494-509, 2016.
- [19] D. Sera, L. Mathe, T. Kerekes, S. V. Spataru, and R. Teodorescu, "On the perturb-and-observe and incremental conductance MPPT methods for PV systems," *IEEE journal of photovoltaics*, vol. 3, no. 3, pp. 1070-1078, 2013.
- [20] J. Kennedy and R. Eberhart, "Particle swarm optimization," in *Proceedings of ICNN'95-international conference on neural networks*, 1995, vol. 4: IEEE, pp. 1942-1948.
- [21] A. Khare and S. Rangnekar, "A review of particle swarm optimization and its applications in solar photovoltaic system," *Applied Soft Computing*, vol. 13, no. 5, pp. 2997-3006, 2013.
- [22] K. V. G. Raghavendra *et al.*, "A comprehensive review of DC-DC converter topologies and modulation strategies with recent advances in solar photovoltaic systems," *Electronics*, vol. 9, no. 1, p. 31, 2019.
- [23] R. B. Gonzatti, Y. Li, M. Amirabadi, B. Lehman, and F. Z. Peng, "An overview of converter topologies and their derivations and interrelationships," *IEEE Journal of Emerging and Selected Topics in Power Electronics*, vol. 10, no. 6, pp. 6417-6429, 2022.
- [24] R. Ayop and C. W. Tan, "Design of boost converter based on maximum power point resistance for photovoltaic applications," *Solar energy*, vol. 160, pp. 322-335, 2018.
- [25] H. Tarzamni, H. S. Gohari, M. Sabahi, and J. Kyyrä, "Non-isolated high step-up dc-dc converters: comparative review and metrics applicability," *IEEE Transactions on Power Electronics*, 2023.